Vibrational spectra of vitreous SiO_2 and vitreous GeO_2 from first principles

2007 J. Phys.: Condens. Matter 19 415112

(http://iopscience.iop.org/0953-8984/19/41/415112)

IOP PUBLISHING JOURNAL OF PHYSICS: CONDENSED MATTER

J. Phys.: Condens. Matter **19** (2007) 415112 (9pp) doi:10.1088/0953-8984/19/41/415112

Vibrational spectra of vitreous SiO_2 and vitreous GeO_2 from first principles

Luigi Giacomazzi[1] **and Alfredo Pasquarello**

Ecole Polytechnique Fédérale de Lausanne (EPFL), Institute of Theoretical Physics, CH-1015 Lausanne, Switzerland
and
Institut Romand de Recherche Numérique en Physique des Matériaux (IRRMA), CH-1015 Lausanne, Switzerland

E-mail: giacomaz@ictp.it and Alfredo.Pasquarello@epfl.ch

Received 27 April 2007
Published 27 September 2007
Online at stacks.iop.org/JPhysCM/19/415112

Abstract

Using a density-functional approach, we calculate the principal vibrational spectra of vitreous SiO_2 and vitreous GeO_2 and discuss their analogies and differences. For both glasses, we generate model structures consisting of a random network of corner-sharing tetrahedra and differing only by their packing density. The comparison between calculated and measured neutron structure factors supports the validity of our model structures. Our investigation then extends to the vibrational properties, including the inelastic-neutron, infrared, and Raman spectra. For these spectra, good agreement with experiment is also found. Our results support the picture that silica and germania are constituted by a continuous random network of corner-sharing tetrahedra. In particular, the good agreement with experiment for the Raman spectra supports the average intertetrahedral angles of 148° and 135° found in our models of vitreous SiO_2 and vitreous GeO_2, respectively. The concentration of small ring structures in these glasses is also discussed.

1. Introduction

Disordered oxides, such as vitreous silica (v-SiO_2) and vitreous germania (v-GeO_2), are currently key materials in many technological applications, ranging from optical fibres [1] to Si-based microelectronic devices [2]. The structure of both v-SiO_2 and v-GeO_2 is generally pictured as a continuous random network of corner-sharing tetrahedra, with the cation at their centre and the O atoms at their corners. However, the two networks are characterized by different packing densities of tetrahedra, with a higher one in v-GeO_2 than in v-SiO_2 [3].

[1] Present address: The Abdus Salam International Centre for Theoretical Physics (ICTP) and CNR-INFM/Democritos National Simulation Center, Strada Costiera 11, I-34100, Trieste, Italy.

This difference affects in particular medium-range properties like the average intertetrahedral bond angle. Indeed, several experimental results indicate that this is significantly lower in v-GeO_2 (133° [4]) than in v-SiO_2 (151° [4, 5]). Other properties affected by the different packing densities are the ring statistics. The concentration of three- and four-membered rings is expected to be higher in vitreous germania than in vitreous silica [6, 7].

Modelling the structure of glassy systems [8] beyond their basic structural unit constitutes a notoriously difficult issue. In addition to the information on the structure derived from diffraction probes (neutrons, x-rays,...), information about medium-range structural aspects might be acquired from the vibrational spectra. Indeed, it has recently been shown [9, 6] that Raman spectra in disordered oxides are highly sensitive to the oxygen bond angle distribution, thus offering an indirect structural probe for the connections between tetrahedra. This sensitivity is particularly valuable since it specifically highlights medium-range arrangements, which are more difficult to access through diffraction probes. However, extracting structural information from vibrational spectra is not trivial and can occur only through accurate modelling, because of the complexity of the involved vibrations and coupling factors. An appropriate theoretical approach should meet several requirements. First, viable model structures need to be generated. Simulation approaches of varying level of complexity are used to this end. For instance, for v-SiO_2 and v-GeO_2, classical molecular dynamics simulations yield model structures which generally compare well with diffraction data [10–12]. In principle, further structural refinement could be achieved with *ab initio* methodologies. However, as far as the vibrational properties are concerned, classical modelling approaches are generally not sufficiently accurate [13, 14]. Furthermore, the modelling of infrared and Raman coupling factors requires an explicit treatment of the electronic structure. An additional constraint results from the necessity of treating model systems of relatively large size in order to describe the disordered nature of the oxide in an appropriate statistical way.

In this work, we present a first-principles investigation of the vibrational spectra of vitreous silica and vitreous germania, and discuss their analogies and differences. We generate model structures by using classical and first-principles methodologies in sequence. Their structural properties are supported by the good agreement with neutron diffraction data [15, 16]. The good agreement with experiment also extends to the vibrational properties. In particular, for both glasses, we carry out comparisons between calculated and measured inelastic-neutron, infrared, and Raman spectra. The sensitivity of the Raman spectra to the intertetrahedral angle provides support to the medium-range properties of our models. Our models of v-SiO_2 and v-GeO_2 feature average Si–O–Si and Ge–O–Ge angles of 148° and 135°, respectively. While the concentration of small ring structures in v-SiO_2 is very low [9], our analysis supports a more sizeable concentration of such rings in v-GeO_2.

2. Methods

The electronic structures were treated within density-functional theory (DFT). For v-SiO_2 and v-GeO_2, we used the local density approximation (LDA) and a generalized gradient approximation (GGA) [17], respectively. Core–valence interactions were described through norm-conserving pseudopotentials for Si and Ge [18, 19] and an ultrasoft one for O [20]. For v-SiO_2, we used plane-wave basis sets with energy cutoffs of 25 and 200 Ryd to expand the electron wavefunctions and the electron density, respectively. For v-GeO_2, we used an energy cutoff of 24 Ryd to expand the electron wavefunctions and of 250 Ryd to expand the electron density. The Brillouin zone was sampled at the Γ point. We derived the vibrational frequencies and eigenmodes from the dynamical matrix, which was calculated numerically by taking finite differences of the atomic forces [13]. For accessing the infrared and Raman spectra, we took

advantage of a recently developed scheme for applying finite electric fields in periodic cell calculations [21]. We obtained the relevant coupling tensors by numerically calculating first and second derivatives of the atomic forces with respect to the electric field [22]. We applied fields of ± 0.005 and ± 0.01 au for v-SiO_2 and GeO_2, respectively. A detailed description of our method to calculate infrared and Raman coupling tensors is given in [22] and [38].

3. Model generation

As a starting point for the generation of our model of v-SiO_2, we selected a model structure among those previously generated by classical molecular dynamics [23, 10] in [24]. We then performed a structural optimization of this model through damped first-principles molecular dynamics [25–27]. This model contains 144 atoms in a periodically repeated cubic cell and shows the experimental density of 2.2 g cm^{-3}.

The model structure of v-GeO_2 was generated as follows. First, classical molecular dynamics simulations [23] of SiO_2 were carried out at the experimental packing density of tetrahedra in v-GeO_2. Through a quench from the melt, we obtained a glassy structure consisting of a chemically ordered network of corner-sharing tetrahedra. A model of v-GeO_2 was then obtained by rescaling the simulation cell by the Ge–O/Si–O bond-length ratio and by further optimizing the atomic positions through damped first-principles molecular dynamics. The final model consists of 168 atoms in a periodically repeated cubic cell at the experimental density of v-GeO_2 (3.65 g cm^{-3} [3]).

4. Structural properties

Our model of v-SiO_2 shows an average bond length ($\sim$1.6 Å) in good agreement with experimental estimates [4]. The tetrahedral units are well defined, showing an average O–Si–O angle close to the ideal one and a standard deviation of 4.3°. The Si–O–Si angle distribution has an average angle of 148.2° (with a standard deviation of 13.4°), in agreement with the experimental estimate of 148.3° [4]. Our model of v-SiO_2 shows a single three-membered ring and ten four-membered rings. The threefold ring is quasi-planar, as can be inferred from the sum Σ over all bond angles in the ring that gives 698°, only slightly lower than the ideal value of 720°.

In our model of v-GeO_2, the average Ge–O bond length (1.78 Å) is only slightly larger than the experimental one (1.74 Å [3]), in accord with a general tendency of the GGA [19][1]. The structure shows well-defined tetrahedral units with O–Ge–O angles centred around the ideal value with a standard deviation of 6°. The Ge–O–Ge angle distribution has an average angle of 135° with a standard deviation of 10.6°, in good agreement with parameters extracted from diffraction data (133°, 8.3°) [4]. Our model of v-GeO_2 contains four three-membered and five four-membered rings. The three-membered rings are all quasi-planar, with an average Σ of 696°. The bond lengths and average intertetrahedral angles of our models are summarized in table 1.

In figure 1(a), we show the comparison between the calculated neutron structure factors of our v-SiO_2 model and the experimental data taken from [15]. Similarly, figure 1(b) shows the comparison between the structure factor of our v-GeO_2 model and corresponding experimental data from [16]. For both model structures, we register good agreement with experiment. In particular, our models describe the first sharp diffraction peak, which originates from the intermediate-range order [29]. The agreement beyond the first sharp diffraction peak stems

[1] With the same set-up, we similarly overestimated by 2% the Ge–O bond length of α-quartz GeO_2.

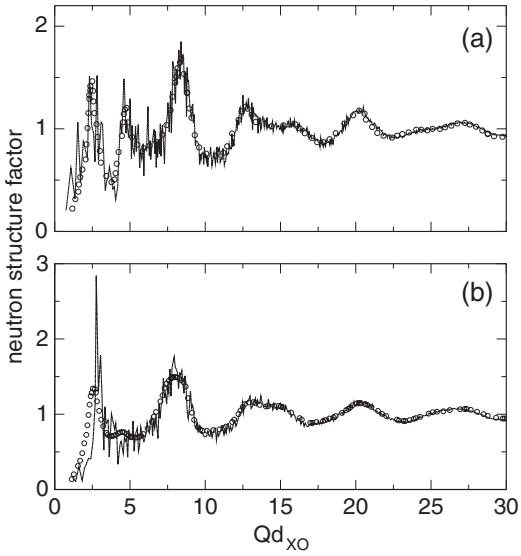

Figure 1. Calculated (solid) and measured (circles) [15, 16] neutron static structure factor of (a) v-SiO_2 and (b) v-GeO_2 at room temperature. We used neutron scattering lengths for O, Si, and Ge of 5.805, 4.149, and 8.185 fm, respectively [28]. The bond lengths in table 1 are used to rescale the transferred momenta.

Table 1. Comparison between structural parameters of v-SiO_2 and v-GeO_2. d_{XO} indicates the bond length and is given in Å. X–O–X (X = Si, Ge) corresponds to the average intertetrahedral angle. Experimental d_{SiO} and d_{GeO} are taken from [4] and [3], respectively. Experimental Si–O–Si and Ge–O–Ge angles are taken from [5] and [4], respectively.

	d_{XO}		X–O–X	
	Model	Expt.	Model	Expt.
v-SiO_2	1.6	1.6	148°	151°
v-GeO_2	1.78	1.74	135°	133°

from the occurrence of tetrahedral units in our model structures. Overall the structure factors of both glasses show features at similar scaled transferred momenta, their modulation being governed by the respective neutron scattering lengths.

5. Inelastic neutron spectra

The reliability of our models of v-SiO_2 and v-GeO_2 also extends to the vibrational properties. In figure 2, the calculated neutron vibrational densities of states [13] of v-SiO_2 and v-GeO_2 are compared to corresponding experimental data of [30, 31] and [32, 33], respectively. Overall, the comparison is very satisfactory, with the theoretical spectra showing all the salient experimental features. In the case of v-GeO_2 (figure 2(b)), the systematic underestimation of the frequencies should be attributed to our DFT set-up [6].

Detailed analyses of vibrational modes reveal that the spectra of silica and germania are composed of three bands [13, 7]. The high-frequency band (above 900 cm^{-1} in v-SiO_2 and above 700 cm^{-1} in v-GeO_2) is mostly given by O stretching motions, with the high-frequency

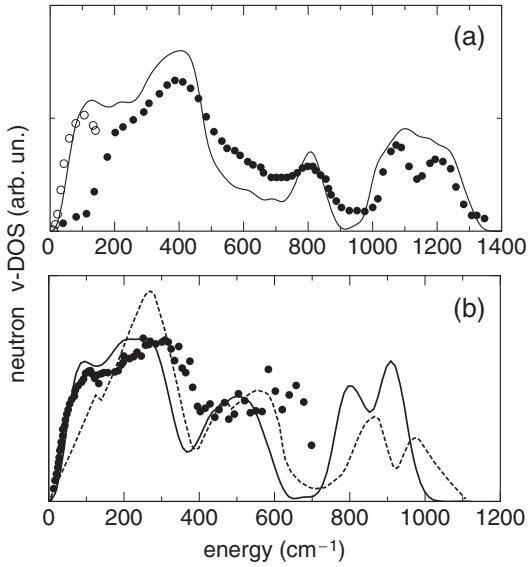

Figure 2. (a) Calculated effective neutron density of states (v-DOS) of our model of v-SiO_2 (solid), compared to experimental results at $T = 33$ K from [30] (closed symbols). Experimental data from [31] are also shown (open symbols). In the calculation, we used transferred momenta in the range 6–13 Å^{-1} [30]. (b) Calculated neutron v-DOS of v-GeO_2 (solid) at room temperature, compared to corresponding experimental data from [32] (discs) and [33] (dashed). The experimental data are scaled with respect to the calculated curve: the former to match the height of the highest peak, and the latter to show the same integrated area. In the calculation, we used transferred momenta in the range 0.5–4.5 Å^{-1} [32].

doublet resulting from tetrahedral modes of different symmetry [13]. The central band is mainly composed of O bending motions while the lowest band predominantly features O rocking motions. The spectrum of v-SiO_2 presents a peak at about 800 cm^{-1} which carries a dominating silicon weight. In the spectrum of v-GeO_2, the corresponding Ge weight has merged with the lower-lying band and does not give rise to a distinct feature. Indeed, because of the large Ge mass, the low band in the spectrum of v-GeO_2 carries a larger cation weight than for v-SiO_2. At low frequencies, the Ge/O ratio approaches 1 in v-GeO_2, whereas the Si/O ratio remains close to the ratio of atomic concentrations. The larger cation mass in v-GeO_2 is also the main cause of the smaller width of the spectrum as compared to v-SiO_2.

6. Infrared spectra

The high-frequency dielectric constants calculated for our models of v-SiO_2 and v-GeO_2 are 2.1 and 2.8, in good agreement with the respective experimental values of 2.1 and 2.6 (table 2). For the static dielectric constants, we obtained 3.8 and 6.3 for v-SiO_2 and v-GeO_2. The value of v-SiO_2 is in excellent agreement with experiment (table 2). We have been unable to find an experimental value for v-GeO_2.

We further investigated the infrared properties through the imaginary part of the dielectric function ϵ_2 [37, 22, 7, 38]. In figures 3(a) and (b), we show the comparison between theory and experiment for ϵ_2 of v-SiO_2 [34] and v-GeO_2 [33], respectively. The theoretical and experimental spectra agree well, in particular for the relative intensities of the main peaks. However, we note that the high-frequency peak of the calculated spectrum of v-

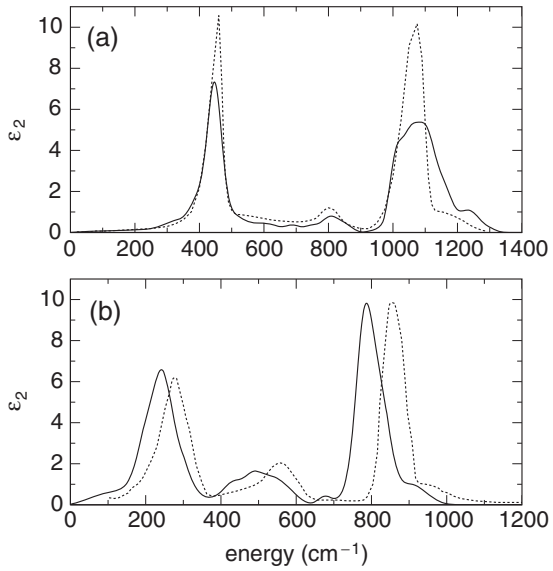

Figure 3. Calculated imaginary part of the dielectric function ϵ_2 (solid) of (a) v-SiO_2 and (b) v-GeO_2, compared with respective experimental spectra of [34] and [33] (dotted). A Gaussian broadening of 19 cm^{-1} is used.

Table 2. Dielectric properties of v-SiO_2 and v-GeO_2: high-frequency (ϵ_∞) and static (ϵ_0) dielectric constants. For v-SiO_2, experimental values of ϵ_∞ and ϵ_0 are taken from [34] and [35], respectively. For v-GeO_2, the experimental value of ϵ_∞ is taken from [36].

	ϵ_∞		ϵ_0	
	Model	Expt.	Model	Expt.
v-SiO_2	2.1	2.1	3.8	3.8
v-GeO_2	2.8	2.6	6.3	

SiO_2 (figure 3(a)) is broader than its experimental counterpart. This effect is related to the width of the bond-length distribution [38, 39] and indicates that the bond-length variations are significantly smaller in the experiment than in the model. We attribute this effect to the excessive strain resulting from the use of periodic boundary conditions in our model. We also remark that the shifts between calculated and measured peak frequencies in the infrared spectrum of v-GeO_2 (figure 3(b)) consistently correspond to those found in the inelastic-neutron spectrum (figure 2(b)). The ϵ_2 of v-SiO_2 and v-GeO_2 appear similar, featuring three main peaks with close relative intensities. This similarity stems from the tetrahedron-based short-range order that the two oxide glasses have in common.

7. Raman spectra

Raman spectra for our models were calculated for incoming and outgoing photons with parallel polarizations (HH). In figure 4(a), the calculated and measured [40] reduced HH Raman spectra of v-SiO_2 are compared. The overall shape of the experimental spectrum is well reproduced by the theory. The agreement is particularly noteworthy for the peak located at 800 cm^{-1}. In figure 4(b), the theoretical reduced HH Raman spectrum of v-GeO_2 is compared with its

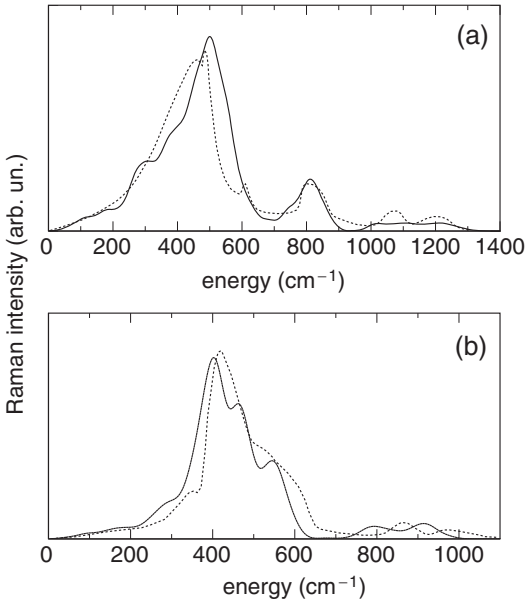

Figure 4. Calculated (solid) HH reduced Raman spectra of (a) v-SiO_2 and (b) v-GeO_2, compared with the corresponding experimental data of [40] and [33] (dotted). The calculated spectra are scaled to match the integrated intensity of the respective experimental spectra. A Gaussian broadening of 19 cm^{-1} is used.

experimental counterpart [33]. The model reproduces well the principal peak and the high-frequency doublet. The overall shift to lower frequencies [6] is consistent with the calculated inelastic-neutron and infrared spectra given above.

The good level of agreement with experiment registered for the inelastic-neutron and infrared spectra stems from the occurrence of regular tetrahedral units in our models and does not shed much light on the network organization beyond nearest neighbours [37, 9, 22]. In contrast, the Raman spectrum is highly sensitive to the X–O–X angle distribution (X = Si, Ge) [9, 7]. Indeed, the HH Raman spectra below 900 cm^{-1} in v-SiO_2 and below 700 cm^{-1} in v-GeO_2 are dominated by O bending motions, which account for about 90% of the integrated intensity. Hence, the agreement between the shape of the calculated and measured HH Raman spectra provides strong support for the X–O–X angle distributions in our model structures.

For v-SiO_2, the Raman spectrum is also informative about the concentration of three-membered and four-membered rings through the intensity of two sharp lines, known as Raman defect lines [41, 9]. In table 3, we compare the concentration of O atoms belonging to three-membered and four-membered rings to estimates derived from the intensity of the Raman defect lines [9]. This comparison shows that the concentration of small rings in our model structure is excessively high. Our model contains a single three-membered ring, but the overall model size needs to be much larger in order to approach the value derived from experiment. The concentration of four-membered rings also exceeds the estimate derived from experiment. A lower concentration of four-membered rings is expected to shift the main peak in figure 4(a) to lower frequencies, thereby improving the agreement with the experimental spectrum.

While three-membered and four-membered rings are also expected in v-GeO_2, its experimental Raman spectrum does not show any defect line resembling those of v-SiO_2. The shoulder at ∼530 cm^{-1} has been shown to result from three-membered rings [6, 7], but detailed

Table 3. Concentration of O atoms belonging to three-membered (O_{3R}) and four-membered (O_{4R}) rings in our models of v-SiO_2 and v-GeO_2. For v-SiO_2, the estimates of [9] are derived from the experimental Raman spectrum.

	O_{3R}		O_{4R}	
	Model	Ref. [9]	Model	Ref. [9]
v-SiO_2	3%	0.22%	42%	0.36%
v-GeO_2	11%		17%	

estimates for the concentrations of such rings could not be derived. The agreement between theory and experiment for the intensity in the shoulder region suggests that the concentration of three-membered rings in v-GeO_2 is close to that in our model structure. Four-membered rings were found to contribute to the main peak of the Raman spectrum of v-GeO_2 [6, 7]. It is at present not clear whether the concentration of such rings would affect the Raman spectrum in a sensitive way. The concentration of O atoms in three-membered and four-membered rings as found in our model structure of v-GeO_2 is given in table 3.

8. Conclusion

In conclusion, the present investigation of v-SiO_2 and v-GeO_2 demonstrates the potential of first-principles methods for interpreting vibrational spectra of oxide glasses. Furthermore, such an analysis offers the opportunity to acquire structural information on the network organization beyond nearest neighbours, which is generally difficult to access in disordered systems. In particular, for v-SiO_2 and v-GeO_2, the analysis of the Raman spectra has provided information on the intertetrahedral bond-angle distribution and on the concentration of small ring structures.

Acknowledgments

Support from the Swiss National Science Foundation is acknowledged (Grant No. 200021-103562/1). The calculations were performed on the cluster PLEIADES of EPFL and on the computational facilities of DIT-EPFL, CSEA-EPFL, and the Swiss Center for Scientific Computing.

References

[1] Li T (ed) 1985 *Optical Fibre Communications* vol 1 (Orlando, FL: Academic) p 9
Ainslie B J and Day C R 1986 *J. Lightwave Technol.* **4** 967
[2] Green M L, Gusev E P, Degraeve R and Garfunkel E L 2001 *J. Appl. Phys.* **90** 2057
[3] Wright A C, Etherington G, Desa J A E, Sinclair R N, Connell G A N and Mikkelsen J C Jr 1982 *J. Non-Cryst. Solids* **49** 63
[4] Neuefeind J and Liss K D 1996 *Ber. Bunsenges. Phys. Chem.* **100** 1341
[5] Mauri F, Pasquarello A, Pfrommer B G, Yoon Y G and Louie S G 2000 *Phys. Rev.* B **62** R4786
[6] Giacomazzi L, Umari P and Pasquarello A 2005 *Phys. Rev. Lett.* **95** 075505
[7] Giacomazzi L, Umari P and Pasquarello A 2006 *Phys. Rev.* B **74** 155208
[8] Madden P 2005 *Nature* **435** 35
[9] Umari P, Gonze X and Pasquarello A 2003 *Phys. Rev. Lett.* **90** 027401
[10] Vollmayr K, Kob W and Binder K 1996 *Phys. Rev.* B **54** 15808
[11] Micoulaut M, Guissani Y and Guillot B 2006 *Phys. Rev.* E **73** 031504
Micoulaut M 2004 *J. Phys.: Condens. Matter* **16** L131

[12] Vashishta P, Kalia R K, Antonio G A and Ebbsjö I 1989 *Phys. Rev. Lett.* **62** 1651
Vashishta P, Kalia R K, Antonio G A and Ebbsjö I 1989 *Phys. Rev.* B **39** 6034
[13] Sarnthein J, Pasquarello A and Car R 1997 *Science* **275** 1925
Pasquarello A, Sarnthein J and Car R 1998 *Phys. Rev.* B **57** 14133
[14] Benoit M and Kob W 2002 *Europhys. Lett.* **60** 269
[15] Susman S, Volin K J, Price D L, Grimsditch M, Rino J P, Kalia R K, Vashishta P, Gwanmesia G, Wang Y and Liebermann R C 1991 *Phys. Rev.* B **43** 1194
[16] Sampath S, Benmore C J, Lantzky K M, Neuefeind J, Leinenweber K, Price D L and Yarger J L 2003 *Phys. Rev. Lett.* **90** 115502
[17] Perdew J P, Chevary J A, Vosko S H, Jackson K A, Pederson M R, Singh D J and Fiolhais C 1992 *Phys. Rev.* B **46** 6671
[18] Bachelet G B, Hamann D R and Schlüter M 1982 *Phys. Rev.* B **26** 4199
[19] Dal Corso A, Pasquarello A, Baldereschi A and Car R 1996 *Phys. Rev.* B **53** 1180
[20] Vanderbilt D 1990 *Phys. Rev.* B **41** 7892
[21] Umari P and Pasquarello A 2002 *Phys. Rev. Lett.* **89** 157602
[22] Umari P and Pasquarello A 2005 *Diamond Relat. Mater* **14** 1255
[23] van Beest B W H, Kramer G J and van Santen R A 1990 *Phys. Rev. Lett.* **64** 1955
[24] Bongiorno A and Pasquarello A 2002 *Phys. Rev. Lett.* **88** 125901
[25] Car R and Parrinello M 1985 *Phys. Rev. Lett.* **55** 2471
[26] Pasquarello A, Laasonen K, Car R, Lee C and Vanderbilt D 1992 *Phys. Rev. Lett.* **69** 1982
Laasonen K, Pasquarello A, Car R, Lee C and Vanderbilt D 1993 *Phys. Rev.* B **47** 10142
[27] http://www.quantum-espresso.org/
[28] Neutron scattering lengths and cross sections are taken from: http://www.ncnr.nist.gov/resources/n-lengths/
[29] Price D L, Saboungi M L and Barnes A C 1998 *Phys. Rev. Lett.* **81** 3207
[30] Carpenter J M and Price D L 1985 *Phys. Rev. Lett.* **54** 441
[31] Buchenau U, Prager M, Nücker N, Dianoux A J, Ahmad N and Phillips W A 1986 *Phys. Rev.* B **34** 5665
[32] Pilla O, Fontana A, Caponi S, Rossi F, Viliani G, Gonzalez M, Fabiani E and Varsamis C 2003 *J. Non-Cryst. Solids* **322** 53
[33] Galeener F L, Leadbetter A J and Stringfellow M W 1983 *Phys. Rev.* B **27** 1052
[34] Philipp H R 1998 *Handbook of Optical Constants of Solids* ed D Palik (San Diego, CA: Academic) p 749
[35] Lide D R (ed) 1998 *Handbook of Chemistry and Physics* (New York: CRC Press)
[36] Murthy M K and Ip J 1964 *Nature* **201** 285
[37] Pasquarello A and Car R 1997 *Phys. Rev. Lett.* **79** 1766
[38] Giacomazzi L 2007 *PhD Thesis (EPFL)* http://library.epfl.ch/theses/?nr=3738
Giacomazzi L and Pasquarello A 2007 unpublished
[39] Giustino F and Pasquarello A 2005 *Phys. Rev. Lett.* **95** 187402
[40] Galeener F L 1982 *Solid State Commun.* **44** 1037
[41] Pasquarello A and Car R 1998 *Phys. Rev. Lett.* **80** 5145